Tree Physiology 17, 359–365

Hydraulic architecture and water relations of a flood-tolerant tropical tree, *Annona glabra*

GERHARD ZOTZ,[1,2,3,4] MELVIN T. TYREE[1,2,3] and SANDRA PATIÑO[3]

[1] *USDA Forest Service, 705 Spear Street, Burlington, VT 05402, USA*

[2] *Department of Botany, University of Vermont, Burlington, VT 05405, USA*

[3] *Smithsonian Tropical Research Institute, Apdo. 2072, Balboa, Republic of Panama*

[4] *Present address: Julius-von-Sachs-Institut für Biowissenschaften, mit Botanischem Garten der Universität Würzburg, Lehrstuhl für Botanik II, Mittlerer Dallenbergweg 64, D-97082 Würzburg, Germany*

Received May 28, 1996

Summary Hydraulic architecture parameters, water relation parameters and wood anatomy were studied in roots and shoots of the flood-tolerant tree *Annona glabra* L. on Barro Colorado Island, Panama. Hydraulic conductivity, leaf specific conductivity, and Huber value were similar to the corresponding values for tree species living in non-flooded habitats. The vulnerability of stems to loss of hydraulic conductivity resulting from embolism was low (50% loss of conductivity at −3.3 MPa). The lowest leaf water potential measured in the field was about −1.0 MPa, indicating that *A. glabra* has a large margin of safety from embolism, which may provide protection against rare drought events, or may be an adaptation to brackish mangrove habitats. Low absolute conductivity of roots was compensated for by an increase in the number of roots. More than two-thirds of whole-plant resistance to water flow was located in the roots.

Keywords: flooding, Huber value, hydraulic conductivity, leaf specific conductivity, vulnerability curve.

Introduction

In the lowland tropics of the Americas, vegetation is subject to periodical short-term or long-term flooding (Campbell et al. 1992). Inundation may be local, affecting only the fringes along rivers, or may spread over large areas. Prance (1979) describes several important forest formations characterized by flooding; for example, Várzea or Igapó ecosystems.

The anatomical, physiological, and ecological adaptations of trees living in these areas do not seem to differ from those of temperate-zone trees in similar habitats, which have been studied extensively (e.g., Crawford 1982, Pezeshki 1990, 1994). However, information about the hydraulic architecture of trees affected by inundation is restricted to saltwater mangroves, such as *Rhizophora mangle* L. (Sperry et al. 1988*a*) or cottonwood ecosystems subject to inundations during spring floods (Tyree et al. 1994*a*). To our knowledge, no study has investigated the hydraulic architecture of a tropical freshwater species.

Annona glabra L. is a small tree with a wide geographical distribution in the tropics and subtropics. It grows in periodically and permanently flooded habitats (Croat 1978). In Central Panama, it occurs along rivers, on the shore of Lake Gatun (the water levels of which show annual fluctuations of about 1.5 m (Panama Canal Commission, unpublished data)), and in brackish habitats close to the sea. Its growth habit, with a swollen trunk base and many adventitious roots, the aerenchyma in its roots and lower trunk, and its buoyant fruits and water-dispersed seeds are all adaptations to the flooded habitat. However, physiological adaptation data are not available. The wide geographical distribution of *Annona glabra* and its ecological importance—for example, in the succession around Lake Gatun in Panama (Croat 1978)—make it an ideal species for the study of physiological adaptations of flood-tolerant trees. In this study, we compared the hydraulic architecture parameters of *A. glabra* with those of tree species that are never flooded. We determined the relative importance of roots, shoots and leaves to whole-plant resistance to water flow. We also assessed the vulnerability of *A. glabra* to cavitation, and compared the resistance of *A. glabra* to stress-induced embolism in the laboratory with the severity of water stress observed *in situ*.

Materials and Methods

Field site and study organism

Investigations were conducted in the Republic of Panama on Barro Colorado Island (BCI) and on some adjacent islands (9°10′ N, 79°51′ W). The tropical moist forest of this biological reserve receives about 2600 mm of precipitation annually, with a pronounced dry season from late December to April (Croat 1978, Leigh et al. 1982).

Annona glabra L. (Annonaceae) is a small tree restricted to swamps, margins of lakes and rivers, and salt marshes. The majority of *A. glabra* trees are flooded for most of the year, and some are permanently inundated. *Annona* trees have a charac-

teristically swollen trunk base below the high water level. The crown of *A. glabra* is very sparse, so most leaves are fully exposed. The species occurs in South America (from Mexico to Brazil), in Africa and in Australia (introduced and naturalized) (Croat 1978, Swarbrick 1993, Swarbrick and Skarratt 1994). Around BCI, it is often found in association with the fern *Acrostichum aureum* L. (Croat 1978).

Field measurements

Gas exchange During the dry seasons of 1994 and 1995, measurements of stomatal conductance, g_w, and water vapor flux density, E, were performed on fully developed leaves of several *A. glabra* trees with a CO_2/H_2O-porometer system (CQP 130, Walz, Effeltrich, Germany) operating in an open-flow mode (see Zotz et al. 1997). The equipment was set up in a boat close to the study site. Ambient air from within the crown was passed through the leaf chamber. The length of the tubing between the leaf chamber and infrared-gas analyzers was approximately 3 m. External temperature was tracked inside the leaf cuvette, and photosynthetic photon flux density (PPFD) was measured close to the leaf with a quantum sensor (LI-190 SA, Li-Cor Inc., Lincoln, NE). Water vapor exchange was measured with a gas analyzer operating in differential mode (BINOS 100, Rosemount, Hanau, Germany). Data were collected for a different tree on each of six days. On a given day, measurements for 3–4 leaves were taken at intervals of 20–50 min between dawn and dusk, and 3–5 h during the night. Individual measurements lasted only a few minutes. Gas exchange parameters were calculated as described by von Caemmerer and Farquhar (1981). Diel curves of PPFD and transpiration were integrated with a digitizing tablet.

Leaves similar to those used for gas exchange measurements were excised at intervals of 60–120 min during the day, and were immediately measured in a pressure chamber to obtain estimates of mean leaf water potential, Ψ_L. Three to four leaves were measured for each tree.

High-pressure flow meter The resistance of leaves and petioles to water flow was assessed with a high pressure flowmeter (Tyree et al. 1993). Briefly, a branch was harvested, connected to the flowmeter and perfused at a pressure of 0.4–0.6 MPa until leaves were completely filled with water. The whole shoot resistance was then computed as (applied pressure × total leaf area)/flow rate (see Yang and Tyree 1994). Subsequently, leaves (including petioles) were removed and the resistance was measured again. The difference between the two resistance measurements was interpreted as the leaf resistance. The experiment was repeated with a total of six branches (basal diameter 7.6–11.5 mm, length 46–102 cm, leaf area 0.09–0.18 m^2) from six different trees.

Laboratory measurements

Hydraulic architecture Four branches (27–41 mm basal wood diameter and 1.6–3.0 m long) of four *A. glabra* trees were harvested, transported to the laboratory and recut under water. Stem segments were cut at various points on the branch, and wood diameter, D, segment length, L, and total leaf area, A_L (measured with a leaf area meter (LI-3100, Li-Cor Inc.)), were recorded for each segment. Twenty-two root segments were collected from four trees. The selected roots were located at water depths of 40–70 cm, either just above or just below the soil surface. Root diameters ranged from 3.4 to 38 mm.

Stem and root segments were placed in a conductivity apparatus (Sperry et al. 1988*b*) which measured the rate of flow of solution (w, kg s^{-1}) in response to the pressure difference (ΔP, MPa). Initial hydraulic conductivity, which is a measure of the absolute hydraulic conductivity of the segment was measured at ΔP = 4–6 kPa, and calculated from:

$$K_h = wL/\Delta P. \quad (1)$$

Specific hydraulic conductivity, K_s, is a measure of the hydraulic efficiency of the xylem in relation to the cross sectional area of wood (A_w). It was calculated as follows:

$$K_s = K_h/A_w, \quad (2)$$

where A_W included functional and nonfunctional wood; i.e., sapwood and heartwood, respectively.

Leaf specific hydraulic conductivity, K_L, provides information about the hydraulic sufficiency of a stem segment on a leaf area basis, and was calculated from:

$$K_L = K_h/A_L. \quad (3)$$

From K_L, the pressure gradient, dP_x/dx, needed in the stem segment to maintain an average evaporative flux density, E, in the leaves to the apex of the segment can be calculated:

$$dP_x/dx = E/K_L. \quad (4)$$

A hydraulically sufficient stem has a high K_L and a low dP_x/dx.

Hydraulic map A hydraulic map was constructed for a small tree cut close to the base. The basal diameter was 104 mm, the length of the shoot was 5.1 m, and the total leaf area was 1.7 m^2. A detailed map of the branching structure was made to allow the calculation of P_x within the stems. The branch was cut into 64 segments, with all cuts made at branch insertion points. The following data were collected for each segment: (1) segment number (starting with 1 at the base), (2) segment number to which the segment was attached at its base, (3) wood diameter of the segment, (4) segment length, and (5) leaf area of the segment. For apical branch segments bearing leaves, the length measured was the distance from the base of the segment to the midpoint of the portion of the segment bearing leaves. Diameters were measured beyond the swelling of the branch insertions.

Vulnerability curves To assess the vulnerability of stem segments to cavitation, we conducted a series of measurements to determine K_h, as described above. Segments were then flushed for 10 min with a degassed solution under a pressure of 150 kPa to dissolve air bubbles in embolized vessels. After flushing, K_h was determined again. The process was repeated until a maximum conductivity, K_m, was achieved (typically after two

flushes). Percent loss of hydraulic conductivity (PLC) was computed from:

$$PLC = 100(K_m - K_h)/K_m. \quad (5)$$

A vulnerability curve is a plot of PLC versus the water stress that induced the PLC. Vulnerabilities were measured by the positive-pressure method (Cochard et al. 1992). Branches 0.5–0.6 m long were collected, the leaf blades removed at the apex of the petioles, and the stem enclosed in a pressure chamber with the base protruding through a rubber seal. Branches were pressurized for 5–12 h at gas pressures ranging from 0.7 to 5.4 MPa. After each branch had been pressurized, it was removed from the chamber and placed under water. Segments 20–30 mm in length and 1.5–3.5 mm in diameter were excised from the branch, all bark was stripped and PLC was determined as described by Cochard et al. (1992).

Vessel dimensions Vessel length distributions were measured on three stems with a wood diameter of 5–22.5 mm by the perfusion method (Zimmermann and Jeje 1981). Briefly, a dilute paint pigment with particle diameters of 1–5 µm (measured by light microscopy) was perfused through the stem segments (length about 1–1.5 m). The particles entered the cut vessels and traveled downstream until they were stopped by pit membranes at the vessel ends. After drying, the stems were cut into consecutive segments of 20 mm each, and the number of paint-filled vessels in each segment counted. Based on Zimmermann's DD algorithm and the algorithm for correction of negative values, the actual vessel distribution was derived from the vessel counts (for detailed discussion, see Tyree 1993).

The number of functioning vessels was determined in stem and root segments (diameters about 6 mm and 12 mm, respectively) by perfusing small branch and root segments with a 0.1% (w/w) Safranin solution. Segments were cut 2 cm from the perfusion end, and the dyed vessels were counted. Vessel diameters in the segments used for vessel counting were measured with the aid of a microscope. Fifty vessels were measured on each of 20 segments.

Miscellaneous measurements Mature leaves were collected for the determination of leaf weight/leaf area ratios (g m^{-2}) and leaf water content (g m^{-2}). Fresh leaves were weighed and leaf area was determined with an LI-3100 leaf area meter. Leaves were then dried for 48 h at 60 °C and weighed again. For six other leaves, the stomatal density was determined by means of nail polish imprints. For the determination of the specific wood density, four root and four shoot segments of similar diameter (2–3 cm) were collected from four different trees. After removal of the bark and determination of volume, the eight samples were dried to constant weight at 60 °C. The specific weight was defined as dry weight per unit volume.

Results

Leaf and wood characteristics

Table 1 shows some important characteristics of mature leaves of *A. glabra*. The leaves are typical mesophylls (Vareschi 1980). The wood of *A. glabra* had a relatively low density, with large differences between branches (0.51 ± 0.04 $g_{DW}\,cm^{-3}$, n = 4) and roots (0.12 ± 0.02 $g_{DW}\,cm^{-3}$, n = 4) of similar size (diameter 2–3 cm). The low specific weight of roots was mostly a result of the well-developed aerenchyma. Vessel length distributions are shown in Figure 1, and vessel density and diameters are given in Table 2. Vessel length was determined in branches of three different sizes. Almost 85% of all vessels were shorter than 10 cm (Figure 1), and the longest vessel was 52 cm in length. Roots had fewer and smaller vessels than shoots (Table 2). For example, roots with a diameter of about 7 mm had 27% the number of vessels found in shoots of similar diameter, and the vessels in roots were about 15% smaller in diameter than in shoots.

Transpiration and leaf water potential

Diel changes in transpiration and leaf water potential were studied on six days. Figure 2 shows a representative 24-h course of leaf transpiration and microclimatic parameters for *A. glabra* in the early dry season of 1995. *Annona glabra* is a small tree; adult trees around Barro Colorado Island are typically between 4 and 7 m tall. Nevertheless, shading by neighboring plants is limited because *A. glabra* grows along the lake shore and is often separated by several meters from the non-

Table 1. Leaf parameters of mature leaves of *A. glabra*. Stomatal density refers to the density on the lower leaf surface. Data are means ± SD; n = number of leaves measured.

Leaf parameter	Mean ± SD	n
Weight/area ratio (g m^{-2})	102.7 ± 10.6	10
Water content (% DW)	210.0 ± 17	10
Water content (g m^{-2})	215.7 ± 20.8	10
Stomatal density (mm^{-2})	432.0 ± 43	10
Thickness (mm^2)	0.36 ± 0.02	10
Area (cm^2)	29.7 ± 12.3	100

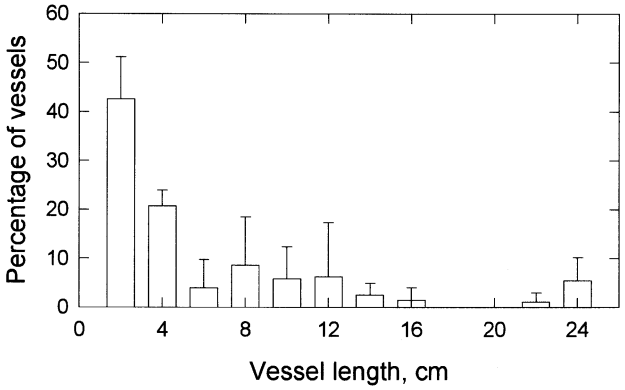

Figure 1. Distributions of vessel lengths in branches of *A. glabra*. Each bar represents the percentage of vessels in a 2-cm size class. Error bar length is SD (n = 3). Only 1% of all vessels were longer than 24 cm. The longest vessels (< 0.1%) were 50–52 cm in length.

Table 2. Vessel width and density in branches and roots of *A. glabra*. Data are means ± SD. Vessel density was determined on five root and five shoot segments, and vessel width was determined for 50 vessels per segment. Differences between shoots and roots were significant for both width and density (*t*-test, ** = $P < 0.01$, *** = $P < 0.001$).

Segment diameter (mm)	Vessel width (μm)		Vessel density (mm^{-2})	
	Shoots	Roots	Shoots	Roots
6.4–7.4	48.8 ± 19.8	43.6 ± 21.9**	16.3 ± 2.4	4.5 ± 1.1***
11.7–12.2	64.6 ± 21.3	48.2 ± 19.6***	14.2 ± 3.1	2.9 ± 0.8***

flooded vegetation. As shown in Figure 2, the average PPFD was about 1500 μmol m^{-2} s^{-1}, with peaks close to 2000 μmol m^{-2} s^{-1}. Stomatal conductance, g_w, and transpiration, *E*, followed the diurnal pattern of PPFD closely. The highest values of g_w reached 300 mmol m^{-2} s^{-1}, when the maximum rates of *E* (E_{max}) were above 4 mmol m^{-2} s^{-1} for extended periods of time. Typically, E_{max} ranged between 4 and 6 mmol m^{-2} s^{-1} (Table 3). The highest E_{max}, 6.4 mmol m^{-2} s^{-1}, was measured on February 25, 1995. Integrated 24-h water loss was about 100 mol m^{-2} day^{-1} (1800 g m^{-2} day^{-1}).

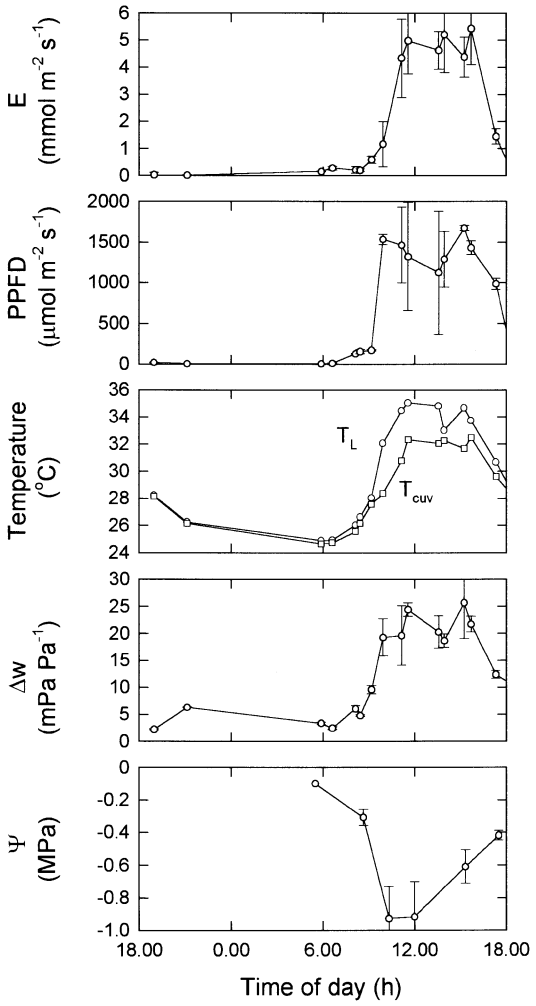

Figure 2. Evaporative flux density (*E*, mmol m^{-2} s^{-1}), microclimatic parameters (PPFD, μmol m^{-2} s^{-1}; leaf temperature (T_L, °C); cuvette temperature (T_{cuv}, °C); and water vapor pressure difference (Δ*w*, MPa Pa^{-1})), and leaf water potential (Ψ_L, MPa) of *A. glabra* measured at Gigante Bay on Barro Colorado Island on February 26, 1995. Data are means ± SD of 3–4 measurements.

Diurnal patterns of leaf water potential (Ψ_L, Figure 2) were the opposite of the patterns in *E*, with the lowest Ψ_L occurring at noon or in the early afternoon. The lowest Ψ_L was about −1 MPa (Table 3). At dusk, values of Ψ_L were typically 0.2 to 0.3 MPa lower than the predawn values.

Hydraulic architecture

Values of initial absolute conductivity, K_h, are plotted versus wood diameter, *D*, in Figure 3. In the range of *D* studied, values of K_h differed by about one order of magnitude between roots and shoots, and were dependent on *D* (Figure 3). Leaf specific conductivity, K_L, also showed a significant dependence on *D* (Figure 3). Smaller stems had a significantly lower K_L than larger stems. All four branches measured showed approximately the same relationship between leaf area, A_L, and basal diameter of the branch bearing the leaves (Figure 3). The Huber value (ratio of wood cross section per unit leaf area) did not change significantly with *D* (R^2 = 0.01, *P* = 0.64). The average Huber value was $3.5 \times 10^{-4} \pm 1.3 \times 10^{-4}$ (*n* = 59).

The vulnerability curve, for *A. glabra* is shown in Figure 4. All measurements were done on segments 1.5–3.5 mm in diameter, just below the leaf-bearing portion of the branch. Native-state loss of conductivity was about 20%, but a greater loss of hydraulic conductivity occurred at a P_x of more than

Table 3. Diel budgets of photosynthetic photon flux density (PPFD, mol m^{-2} day^{-1}) and diel evaporative leaf water loss (*E*, mol m^{-2} day^{-1}), estimated from gas exchange measurements *in situ*. Also given are the maximum rate of transpiration (E_{max}, mmol m^{-2} s^{-1}) and the mimimum leaf water potential (Ψ_{Lmin}, MPa). Data are means for PPFD and *E*, and means ± SD (*n* = 3–4) for E_{max} and Ψ_{Lmin}; nd = not determined.

Date	PPFD	*E*	E_{max}	Ψ_{Lmin}
Jan 15, 1994	33.7	107.1	5.2 ± 0.5	nd
Mar 6, 1994	10.0	40.1	2.1 ± 0.1	−1.1 ± 0.1
Mar 30, 1994	7.2	nd	nd	−1.1 ± 0.1
Jan 7, 1995	37.3	98.1	4.3 ± 2.8	−0.8 ± 0.1
Feb 25, 1995	30.9	90.3	6.4 ± 0.3	−1.2 ± 0.1
Feb 26, 1995	31.4	104.9	5.4 ± 1.3	−0.9 ± 0.2

1.5 MPa. Values of PLC of 50 and 80% were reached at 3.3 and above 5.0 MPa, respectively.

Figure 5 shows pressure profiles of three randomly selected conducting paths from the base of a small tree to leaf-bearing twigs. The pressure drop was calculated for a transpiration rate of 4 mmol m^{-2} s^{-1}, and included a gravitational component of −0.01 MPa m^{-1}. Most of the pressure drop occurred in the smaller branches (path length > 3m). The pressure drop in stem segments with larger diameters primarily resulted from the gravitational potential. The calculation did not include leaf resistance (R_L). To determine R_L, we used a high-pressure flow meter (Tyree et al. 1993). Based on an average leaf resistance of $3.8 \times 10^{-2} \pm 1.5 \times 10^{-2}$ MPa s m^2 $mmol^{-1}$ (mean ± SD, n = 6), we estimated the necessary pressure drop across the leaf to be about 0.15 MPa. The entire pressure drop from the base of this 5-m tall tree to the transpiring surfaces was thus estimated to be about 0.3 MPa.

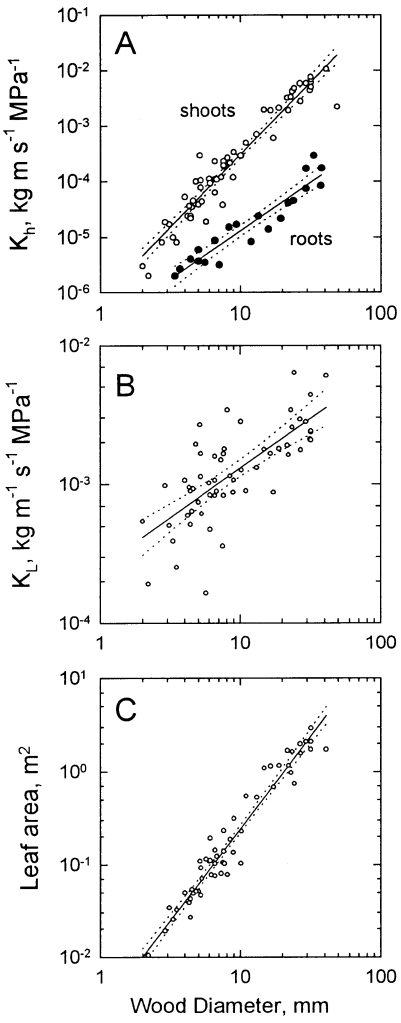

Figure 3. (A) Initial absolute conductivity, K_h, of *A. glabra* shoot segments (open circles) and root segments (closed circles) versus wood diameter. Values are presented as log-log plots. Straight lines are linear regressions and dotted lines are 95% confidence intervals. Linear regression equations are: shoots: $\log(k_h) = -6.2 + 2.7 \log(D)$, R^2 = 0.94, $P < 0.001$; roots: $\log(k_h) = -6.6 + 1.7 \log(D)$, $R^2 = 0.92$, $P < 0.001$. (B) Leaf specific conductivity, K_L, versus stem diameter measured on the segments used in panel A. The linear regression is: $\log(K_L) = -3.6 + 0.7 \log(D)$, $R^2 = 0.54$, $P < 0.001$. Dotted lines are 95% confidence intervals. (C) Comparison of leaf area and basal wood diameter of a branch. Values are from four different trees. The regression equation is: $\log(A_L) = 1.4 + 2.0 \log(D)$, $R^2 = 0.95$, $P < 0.001$. Dotted lines are 95% confidence intervals.

Discussion

Most of the whole-plant resistance to water flow in *A. glabra* was located in the roots and possibly in the swollen transition zone between the roots and trunk. The water flow necessary to sustain a leaf transpiration rate of 4 mmol m^{-2} s^{-1} would result in a pressure drop from trunk base to leaf blade of 0.3 MPa (Figure 5). This is only about 30% of the minimum water potential determined in the field (Figure 2, Table 3). Because the plants were all growing in shallow water, we assumed that soil water potential was close to 0 MPa. The leaf water potential thus adequately estimates the driving force for water flow from absorbing root tips to transpiring leaf blades. Therefore, two-thirds of the entire resistance to water flow in *A. glabra* is located in the roots. Roots are very different from shoots, both morphologically (Table 2) and functionally (Figure 3). It has been established that flooding affects root function by hampering water uptake (Crawford 1982, Pezeshki 1994). Even in well-adapted species, such as *Alnus glutinosa* (L.) Gaertn., flooding leads to a reduction in Ψ_L (Gill 1975). We did not

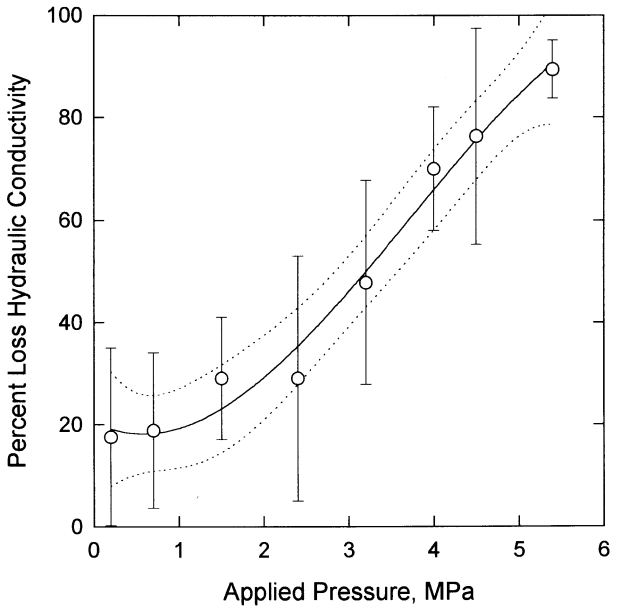

Figure 4. Vulnerability curve for stem segments (diameter 1.5–3.5 mm) of *A. glabra*. Percent loss hydraulic conductivity (PLC) is plotted versus the pressure causing the observed PLC. Applied pressure (on the *x*-axis) refers to the pressure applied in a pressure bomb to dehydrate branches before stem segments were excised under water. Each point is the mean for 8 to 10 stem segments; error bars indicate SD. The solid line is the best fit third-order polynomial regression with 95% confidence limits (dotted lines).

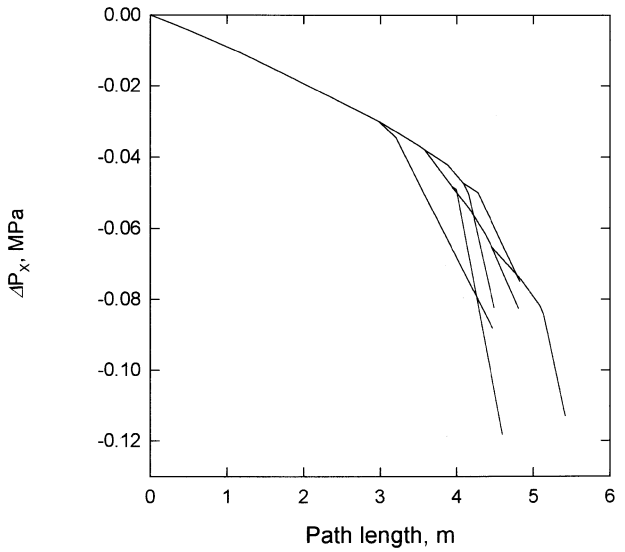

Figure 5. Pressure potential profiles, calculated from a hydraulic map, for steady-state flow of water through a small *A. glabra* tree. The *y*-axis gives the change in pressure potential (ΔP_x) from the base of the branch to any given point along the branch. The *x*-axis is the distance along the trunk and branches (m). The pathways from the base of the branch to six different apices were randomly selected and plotted. The average evaporative flux density, *E*, of leaves used for calculations was 4 mmol m^{-2} s^{-1}. Also included is a gravitational potential of −0.01 MPa m^{-1} height.

measure water uptake of *A. glabra* roots directly, and could not estimate the importance of radial versus axial resistance to water flow in roots. In general, the resistance along the axis of roots is assumed to be lower than the radial resistance (Frensch and Steudle 1989, Tyree et al. 1994*b*). However, the low K_h of *A. glabra* roots (Figure 3) suggests that a considerable portion of the whole-root resistance to water flow is caused by the axial component.

In anoxic soils, the development of aerenchyma for the aeration of roots counteracts the root function as an efficient conducting system. One way of compensating for this inefficiency would be to develop a massive root system, which also ensures mechanical support of the tree in an unstable substrate; and, in fact, root biomass can exceed shoot biomass in mature *A. glabra* (unpublished data).

Anoxic soils allow only shallow rooting (< 30 cm depth, unpublished data). Thus, *A. glabra* trees may suffer severe drought stress quickly when their growing sites occasionally dry out. The high resistance to embolism (Figure 4) might be an adaptation to such events. It is also conceivable that low vulnerablity is part of the adaptation of this species to brackish habitats. The apparent deviation from the general pattern that severity of stress *in situ* and resistance to cavitation correlate quite closely (Tyree et al. 1994*c*), needs further analysis.

The hydraulic efficiency of the trunks and branches of the flood-tolerant *A. glabra* falls in the same range as the hydraulic efficiency of tropical and temperate tree species where comparable data are available (Tyree and Ewers 1991, Patiño et al. 1995). Hydraulic parameters were in the lower half of the range of approximately 20 species studied, but all values were close to the median (Table 4). In addition, similar to the results of other studies, e.g., with *Acer saccharum* Marsh. or *Acer rubrum* L. (Yang and Tyree 1994), *A. glabra* leaves and petioles accounted for about half of the whole-shoot resistance to water flow. Thus, we observed no unusual features in the aboveground vascular system of *A. glabra*. On the level of the entire organism, however, the hydraulic system of *A. glabra* is quite efficient, as is indicated by high transpiration rates (Table 3, Figure 2), which are among the highest found in tropical and temperate tree species (Larcher 1994, Zotz et al. 1995).

Table 4. Comparison of hydraulic architecture parameters of *A. glabra* with other tropical and temperate angiosperm trees. Parameters are Huber value (H_v), leaf specific conductivity (K_L), and specific conductivity (K_s), and are standardized for a wood diameter of 15 mm. For the species used for comparison, the range and the median are given and *n* = number of species (Patiño et al. 1994).

Parameter	*A. glabra*	Other species	*n*
H_v ($\times 10^{-4}$)	3.5	0.9–20 (2.1)	18
K_L (kg s^{-1} m^{-1} MPa^{-1} $\times 10^{-3}$)	1.8	0.2–12 (1.8)	20
K_s (kg s^{-1} m^{-1} MPa^{-1})	9.1	1.3–35 (4.8)	18

Acknowledgments

This work was made possible by Cooperative Research agreement number 23-911 between the USDA Forest Service and the University of Vermont for the salary of GZ, and Cooperative Research Agreement number 23-597 between the USDA Forest Service and the Smithsonian Tropical Research Institute for research costs. We thank Dr. O.L. Lange (Würzburg) for the use of his CQP-porometer and Bettina Weber (Würzburg) and Patricia Bermejo (STRI) for help with measurements. We also acknowledge the Panama Canal Comission for the unpublished data on the lake levels of Lake Gatun.

References

Campbell, D.G., J.L. Stone and A. Rosas, Jr. 1992. A comparison of the phytosociology and dynamics of three floodplain (*Várzea*) forests of known ages, Rio Juruá, western Brazilian Amazon. Bot. J. Linn. Soc. 108:213–237.

Cochard, H., P. Cruiziat and M.T. Tyree. 1992. Use of positive pressures to establish vulnerability curves. Plant Physiol. 100:205–209.

Crawford, R.M.M. 1982. Physiological responses to flooding. *In* Physiological Plant Ecology II. Encyclopaedia of Plant Physiology, Volume 12B. Eds. O.L. Lange, P.S. Nobel, C.B. Osmond and H. Ziegler. Springer-Verlag, New York, pp 453–477.

Croat, T. 1978. Flora of Barro Colorado Island. Stanford University Press, Stanford, CA, 943 p.

Frensch, J. and E. Steudle. 1989. Axial and radial hydraulic resistance to roots of maize (*Zea mays* L.). Plant Physiol. 91:719–726.

Gill, C.J. 1975. The ecological significance of adventitious rooting as a response to flooding a woody species, with special reference to *Alnus glutinosa* (L.) Gaertn. Flora 164:85–97.

Larcher, W. 1994. Ökologie der Pflanzen. Ulmer, Stuttgart, 394 p.

Leigh, E.G., Jr., A.S. Rand and D.M. Windsor, Eds. 1982. The ecology of a tropical forest. Seasonal rhythms and long-term changes. Smithsonian Institution Press, Washington, D.C., 468 p.

Patiño, S., M.T. Tyree and E.A. Herre. 1995. Comparison of hydraulic architecture of woody plants of differing phylogeny and growth form with special reference to free-standing and hemi-epiphytic *Ficus* species from Panama. New Phytol. 129:125–134.

Pezeshki, S.R. 1990. A comparative study of the response of *Taxodium distichum* and *Nyssa aquatica* seedlings to soil anaerobiosis and salinity. For. Ecol. Manage. 33/34: 531–541.

Pezeshki, S.R. 1994. Plant response to flooding. *In* Plant–Environment Interactions. Ed. R.E. Wilkinson. Marcel Dekker, New York, pp 289–321.

Prance, G.T. 1979. Notes on the vegetation of Amazonia. III. The terminology of Amazonian forest types subject to inundation. Brittonia 31:26–38.

Sperry, J.S., M.T. Tyree and J.R. Donelly. 1988*a*. Vulnerability of xylem to embolism in a mangrove vs. an island species of Rhizophoraceae. Physiol. Plant. 74:276–283.

Sperry, J.S., J.R. Donelly and M.T. Tyree. 1988*b*. A method for measuring hydraulic conductivity and embolism in xylem. Plant Physiol. 11:35–40.

Swarbrick, J.T. 1993. The biology, distribution, impact and control of five weeds of the wet tropics world heritage area. Wet Tropics Management Agency, Queensland, Australia, 63 p.

Swarbrick, J.T. and D.B. Skarratt. 1994. The ecological requirements and potential Australian distribution of pond apple (*Annona glabra*). Wet Tropics Management Agency, Queensland, Australia, 8 p.

Tyree, M.T. 1993. Theory of vessel-length determination: the problem of nonrandom vessel distribution. Can. J. Bot. 71:297–302.

Tyree, M.T. and F.W. Ewers. 1991. The hydraulic architecture of trees and other woody plants. New Phytol. 119:345–360.

Tyree, M.T., B. Sinclair, P. Lu and A. Granier. 1993. Whole shoot hydraulic resistance in *Quercus* species measured with a new high-pressure flowmeter. Ann. Sci. For. 50:417–423.

Tyree, M.T., K.J. Korb, S.B. Rood and S. Patiño. 1994*a*. Vulnerability to drought-induced cavitation of riparian cottonwoods in Alberta: a possible factor in the decline of the ecosystem? Tree Physiol. 14:455–466.

Tyree, M.T., S. Yang, P. Cruiziat and B. Sinclair. 1994*b*. Novel methods of measuring hydraulic conductivity of tree root systems and interpretation using AMAIZED. Plant Physiol. 104:189–199.

Tyree, M.T., S.D. Davis and H. Cochard. 1994*c*. Biophysical perspectives of xylem evolution: is there a tradeoff of hydraulic efficiency for vulnerability to dysfunction? IAWA J. 15:335–360.

Vareschi, V. 1980. Vegetationsökologie der Tropen. Ulmer, Stuttgart, 293 p.

von Caemmerer, S. and G.D. Farquhar. 1981. Some relationships between the biochemistry of photosynthesis and the gas exchange of leaves. Planta 153:376–387.

Yang, S. and M.T. Tyree. 1994. Hydraulic architecture of *Acer saccharum* and *A. rubrum*: comparison of branches to whole trees and the contribution of leaves to hydraulic resistance. J. Exp. Bot. 45:179–186.

Zimmermann, M.H. and A.A. Jeje. 1981. Vessel-length distribution in stems of some American woody plants. Can. J. Bot. 59:1882–1892.

Zotz, G., M. Königer, G. Harris and K. Winter. 1995. High rates of photosynthesis in the tropical pioneer tree, *Ficus insipida* Willd. Flora 190:265–272.

Zotz, G., S. Patiño and M.T. Tyree. 1997. CO_2 gas exchange and the occurrence of CAM in tropical woody hemiepiphytes. Flora. In press.